MEMS Pirani Sensor for Pressure Measurements in the Fine- and High-Vacuum Range

M. Grau [1,2], F. Völklein [1], A. Meier [1], C. Kunz [1], P. Woias [2]

[1] RheinMain University of Applied Sciences, Institute for Microtechnologies (IMtech), Rüsselsheim, Germany
[2] University of Freiburg, Department of Microsystems Engineering, Freiburg, Germany

Pirani vacuum gauges are commonly used sensors for pressure measurements.

Typical specifications:

- Range: 100 mbar to 10^{-3} mbar
- Advantages: robust, simple in design, cheap in production
- Dimensions: 5x5x10 centimeters in height, width and length

Advantages of miniaturization:

- small size
- extended measuring range
- low power consumption
- batch processing

Reduced size and an extended measuring range enable new application fields like:

- Mass spectroscopy
- Vacuum isolation and process monitoring
- Integration in vacuum pumps
- Pressure measurements during space missions

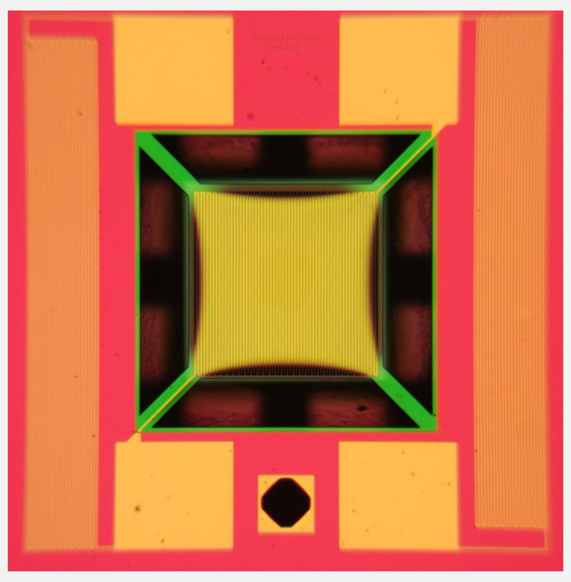

Figure 1. MEMS Pirani chip after anisotropic etching of silicon; the suspended membrane with Ni resistor is carried by four thin beams[1]

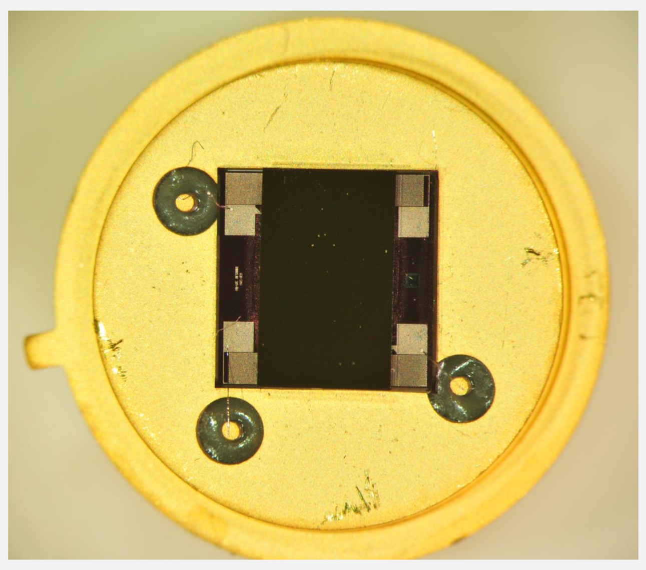

Figure 2. Pirani Sensor VAC_03 for the fine and high vacuum with Pirani Sensor VAC_04 for the rough vacuum on one transistor outline header[1]

Principle: Conventional thermal conductivity vacuum gauges are based on measurements of thermal losses of electrical heated wires due to gas thermal conduction. Heat flux through the surrounding gas depends on pressure and should be maximized to achieve high sensitivity, whereas the heat losses by radiation and solid thermal conduction have to be minimized. A transfer of this measurement principle to silicon based micro-chips allow significant improvements in sensitivity and measuring range.

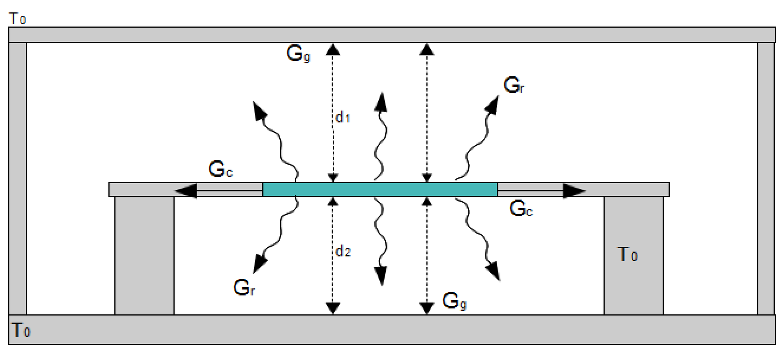

Figure 3. Schematic setup of micropirani sensors

$$\Delta T = \frac{N}{G_c + G_r + G_g(p)} \quad (1)$$

$$U_S \approx \frac{1}{4}\beta \Delta T U_B \quad (2)$$

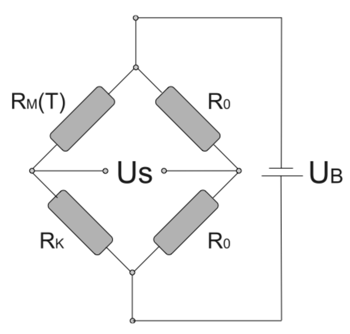

Figure 4. Wheatstone bridge

$$G_c = 4\frac{\lambda_{Si_3N_4} d_M b}{l} + 2\frac{\lambda_{Ni}(T)\, d_{Ni} b_{Ni}}{l} \quad (3)$$

$$G_g \propto \lambda(p, d_1)\frac{A}{d_1} + \lambda(p, d_2)\frac{A}{d_2} \quad (4)$$

$$G_r = \frac{2\varepsilon\sigma(T^4 - T_0^4)A}{T - T_0} \quad (5)$$

$$\lambda(p,d) = \lambda(p_0)\left(1 + 2\left(\frac{2-a}{a}\right)\frac{\bar{l}(p)}{d}\frac{9.5}{6}\right)^{-1} \quad (6)$$

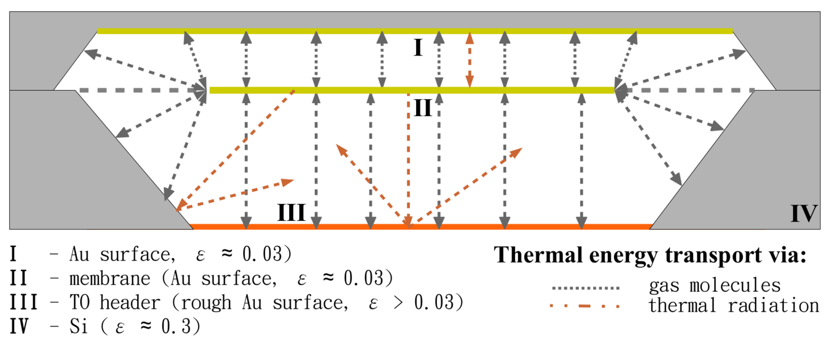

Figure 5. Schematic cross section showing problems in modeling thermal energy transport by gas molecules and radiation

Problems of analytical solutions:

- Varying distances between membrane and walls (4,6)
- Effective emissivity has to be measured (combination of A,B,C) (5)
- No temperature dependency for λ_{Si3N4}; $\lambda_{Ni}(T)$ is calculated by Wiedemann-Franz law(3)
- Energy accommodation coefficients used from literature (6)

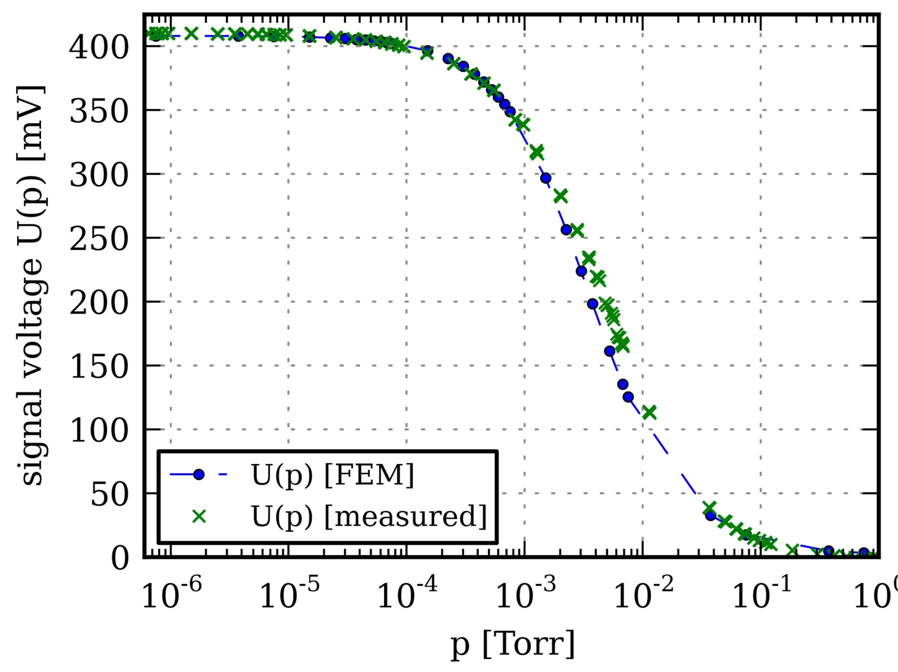

Figure 6. Calculated and measured signal voltage U(p) of the chip type VAC_03 in the fine- and high vacuum range

Figure 7. Parametric sweep of the distance between membrane and silicon microbridge (Si-mb)

Parameter Sweeps
Distances d_1 and d_2
Chip Rim width
Beam length/width
Membrane size
Material properties (TCR, λ)
Bridge supply-voltage

Table 1. List of parametric sweeps

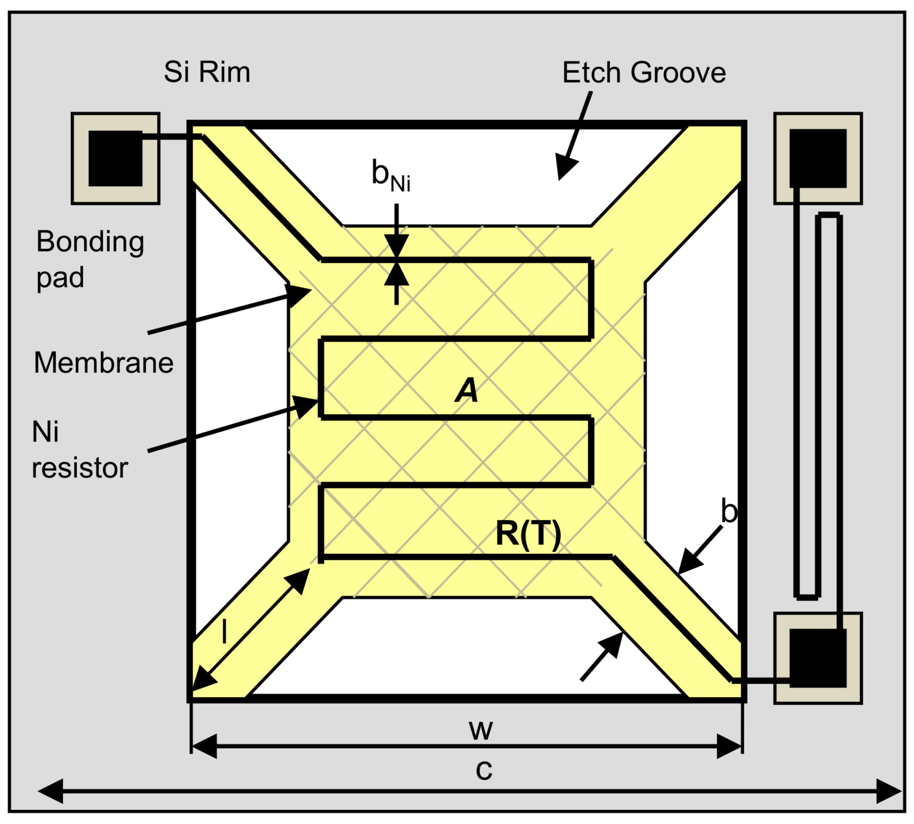

Figure 8. Schematic of the sensor design with a suspended Si_3N_4 membrane above an etched cavity, carried by 4 Si_3N_4 beams.

	VAC_03	units
A	4	mm²
w	3000	µm
l	746	µm
b	70	µm
b_{Ni}	12	µm
d_{Ni}	200	nm
d_M	300	nm

Table 2. Chip dimensions for VAC_03

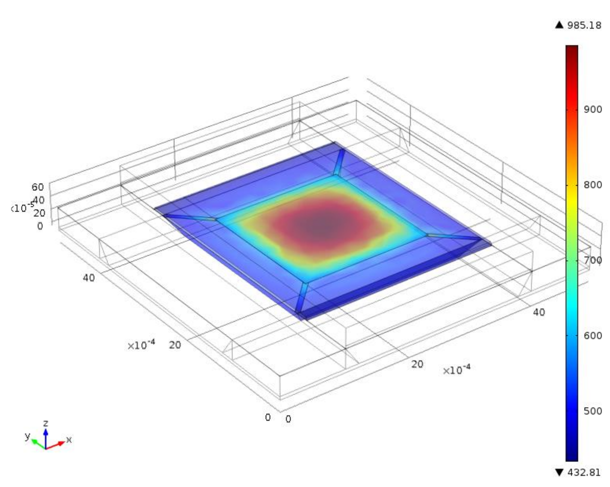

Figure 9a. Radiation losses inside the sensor cavity (silicon microbridge and chip rim fully transparent)

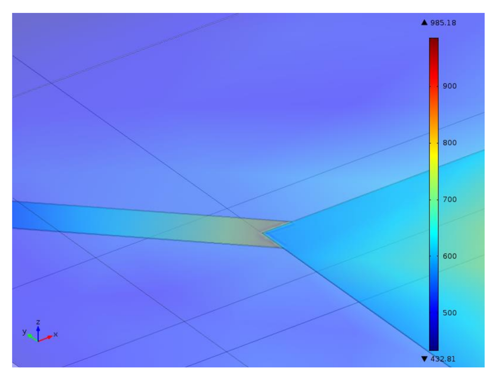

Figure 9b. Radiation losses of and near the membrane and its supporting beams

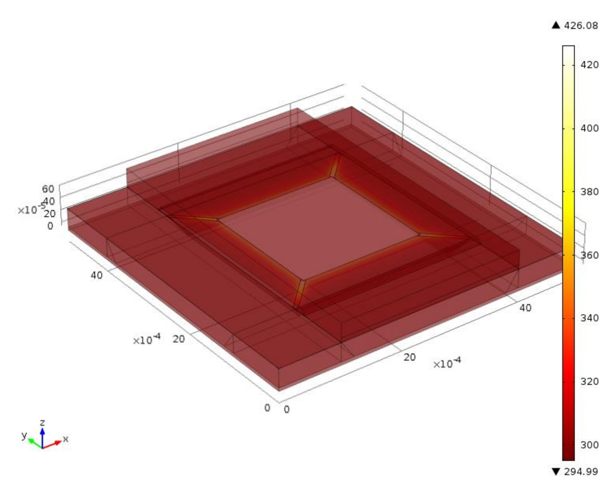

Figure 10. Temperature distribution for pressure p=10^{-7} Torr, on top of the chip-rim a silicon microbridge is placed (semi-transparent)

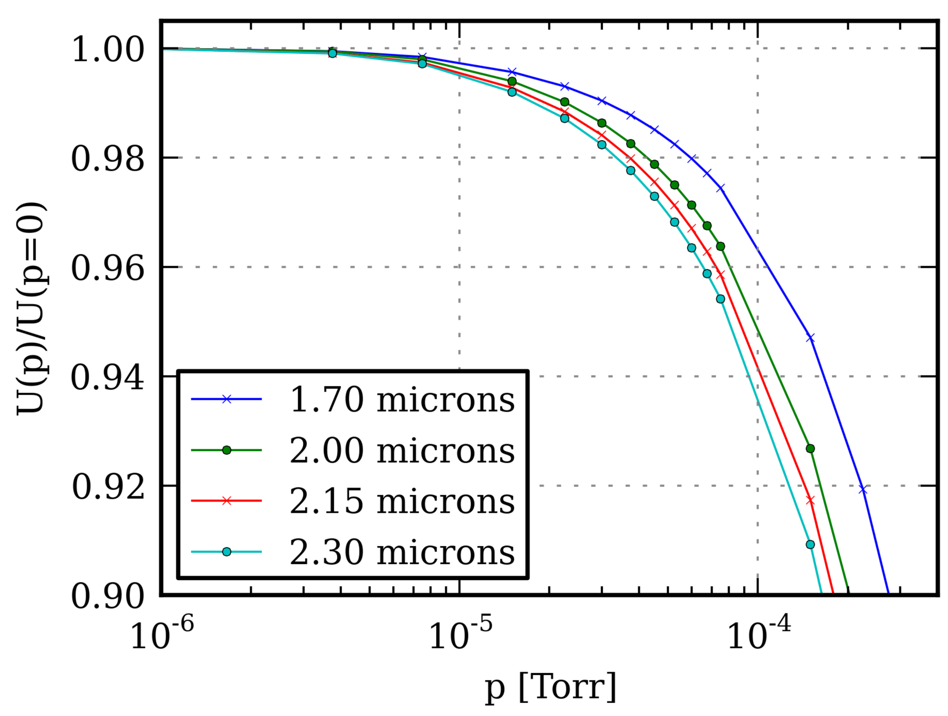

Figure 11. Parametric sweep of membrane's edge length

Computational details and specifications	
COMSOL Version	4.2a
Hardware	Xeon E31225, 16 GB Ram
Number of degrees of freedom	292757
Mesh parts	4
Minimum memory size for solving model	12 GB

Table 3. Computational details and specifications

Mario Grau
mario.grau@hs-rm.de
Hochschule RheinMain

Friedemann Völklein
friedemann.voelklein@hs-rm.de
Hochschule RheinMain

Andreas Meier
andreas.meier@hs-rm.de
Hochschule RheinMain

References: [1]F. Völklein, M. Grau et al., J. Vac. Sci. Technol. A 31, 061604 (2013)

Excerpt from the Proceedings of the 2014 COMSOL Conference in Cambridge